Lien, S., & Racker, E. (1971) *Methods Enzymol. 23*, 547–555.
Magnusson, R. P., Portis, A. R., & McCarty, R. E. (1976) *Anal. Biochem. 72*, 653–657.
McCarty, R. E., & Racker, E. (1966) in *Energy Conservation by the Photosynthesis Apparatus*, No. 19, pp 202–212, Brookhaven National Laboratory, Upton, NY.
McCarty, R. E., & Racker, E. (1967) *J. Biol. Chem. 242*, 3435–3439.
Mitchell, P. (1974) *FEBS Lett. 43*, 189–194.
Penefsky, H. S. (1977) *J. Biol. Chem. 252*, 2891–2899.
Postmus, C., & King, E. L. (1955) *J. Phys. Chem. 59*, 1208–1222.
Selman, B. R., & Durbin, R. D. (1978) *Biochim. Biophys. Acta 502*, 29–37.
Selman, B. R., & Selman-Reimer, S. (1981) *J. Biol. Chem. 256*, 1722–1726.
Shoshan, V., & Selman, B. R. (1979) *J. Biol. Chem. 254*, 8801–8807.
Strotmann, H., Bickel-Sandkotter, S., Edelman, K., Schlimme, E., Boos, K. S., & Lustdorff, J. (1977) *BBA Libr. 14*, 307–317.
Strotmann, H., Bickel-Sandkotter, S., Edelman, K., Eckstein, F., Schlimme, E., Boos, K. S., & Lustdorff, J. (1979) *Biochim. Biophys. Acta 545*, 122–130.
Weber, K., & Osborn, M. (1969) *J. Biol. Chem. 244*, 4006–4412.
Yee, D., & Eckstein, F. (1980) *FEBS Lett. 112*, 10–12.
Young, J. H., Korman, E. F., & McLick, J. (1974) *Bioorg. Chem. 3*, 1–15.

# Compartmental Analysis of Light-Induced Proton Movement in Reconstituted Bacteriorhodopsin Vesicles†

Richard D. Klausner,* Mones Berman, Robert Blumenthal, John N. Weinstein, and S. Roy Caplan

ABSTRACT: Purified bacteriorhodopsin from purple membrane sheets isolated from *Halobacter halobium* was solubilized with a bile salt detergent, 3-[(3-cholamidopropyl)dimethylammonium]-1-propanesulfonate (CHAPS). The detergent-solubilized protein was then incorporated into lecithin vesicles at either high (450:1) or low (65:1) lipid to protein ratios. Circular dichroism studies showed that the bacteriorhodopsin incorporated was in a monomeric form in the 450:1 vesicles. The 65:1 vesicles exhibited an exciton splitting characteristic of the aggregated state of bacteriorhodopsin. We then examined the light-induced movement of protons for these two preparations. Compartmental analysis was used to derive a kinetic model for the observed proton movement. The pumping was qualitatively the same for monomeric and aggregated protein. A three-compartment model provided an excellent description of proton movement in both sets of vesicles and at four different light intensities. This model demands two independent processes to account for the proton movement. The rate coefficients for both are linearly related to light intensity. However, the total flux of protons via one of these processes diminishes as a function of the hydrogen ion accumulation within the vesicles.

For the past decade bacteriorhodopsin (BR) has been an object of intensive study both as a membrane protein whose detailed structure has been extremely amenable to study (Oesterhelt & Hess, 1971; Henderson, 1977) and as a light-driven proton pump (Oesterhelt & Stoeckenius, 1973; Racker & Stoeckenius, 1974; Bogomolni & Stoeckenius, 1974). Information on the photocycle has provided the basis for ideas about the mechanism linking capture of photons to translocation of protons across the membrane. Nevertheless, the exact molecular details of pumping are not known (Slifkin & Caplan, 1975; Marcus & Lewis, 1977). Several groups have reconstituted BR into phospholipid vesicles in order to examine, in controlled lipid environments, the process of light-induced proton movement (Racker, 1973; Hellingwert et al., 1978). By using a detergent dialysis technique, we have reconstituted BR into uncharged phosphatidylcholine vesicles. By variation of the lipid to protein ratio, the resulting vesicles contain either monomeric or multimeric BR as judged by the absence or presence, respectively, of an exciton splitting as determined by circular dichroism (Heyn et al., 1975). We then measured light-induced pumping in order to analyze the kinetics of proton movement over time periods that were long with respect to the photocycle in order to observe the characteristics of the pump under the "physiologic" condition of prolonged irradiation. The purpose of this study is 2-fold: (1) to investigate whether the numerical data on buildup and decay of light-induced pH gradients point to the existence of multiple proton compartments and (2) to determine whether any differences are apparent between the proton pumping of monomeric vs. multimeric BR. Compartmental analysis is used in this study to characterize proton movement. One of the great advantages of compartmental analysis is that it allows an association of discrete processes with each compartment. Previous work by Eisenbach et al. (1978), using a standard fit to sums of exponentials, suggested that two processes are involved in light-induced proton movement. The results of our compartmental analysis support those conclusions and provide an explicit model to explain both the light-induced pH changes and the reversal of those changes when illumination ceases. By examining pH changes as a function of illuminating intensities, we can relate the rate constants of the various processes to the energy input. Recently, proton pumping has been observed in lipid vesicles containing monomeric BR (Dencher & Heyn, 1979). The studies reported here show that the

† From the Laboratory of Theoretical Biology, DCBD, National Cancer Institute, National Institutes of Health, Bethesda, Maryland 20205, and the Department of Membrane Research, Weizmann Institute of Science, Rehovot, Israel. *Received July 7, 1981.*
* Address correspondence to this author at the Laboratory of Theoretical Biology, National Cancer Institute.

mechanims involved in proton movement are similar in both monomeric and multimeric BR vesicles.

## Materials and Methods

Purified sheets of purple membrane were obtained according to previously published methods (Oesterhelt & Stoeckenius, 1971, 1974). These were diluted into a buffer consisting of 150 mM NaCl, 5 mM sodium acetate, and 0.5 mM sodium azide at pH 6.0 at a final concentration of 100 $\mu$M protein. Detergent was added (see below), and the solution was mixed with a magnetic stirring bar for 24 h at room temperature and protected from light. The detergent used in the studies reported here was 3-[(3-cholamidopropyl)dimethylammonium]-1-propanesulfonate (CHAPS). It was synthesized and kindly provided to us by Dr. L. Hjelmeland. Its advantages for this study included its relatively high cmc (5–10 mM) and its lack of optical activity in the visible range.

Egg yolk lecithin was purchased from Sigma and stored in chloroform at −20 °C under argon. A 10-mg sample was dried under argon and lyophilized overnight before use. Before the sample was dried, 1 $\mu$Ci of [$^{14}$C]dipalmitoylphosphatidylcholine (DPPC) (Applied Sciences, 55 mCi/mmol) was added to the egg yolk lecithin. The solubilized protein in 1 mL of buffer was added to the lyophilized lipid and vortex mixed at room temperature for 10 min. The suspension was placed in Spectropore No. 3 dialysis tubing (which had been boiled in buffer) and dialzyed against 1 L of buffer for 4 days at room temperature. The dialysis buffer was changed every 24 h. The sample was protected from light during dialysis. We found that the concentration of detergent was critical to the success of the reconstitution. When either octyl $\beta$-glucoside (cmc 22 mM) or CHAPS (cmc 5–10 mM) was used at twice its cmc, the reconstitution failed. This was obvious in that large lipid vesicles or vesicle aggregates containing no visible purple BR began to settle in the dialysis tubing. The absence of reconstitution could be confirmed by isopycnic density centrifugation, which, in these cases, revealed that all of the lipid banded at a density of 1.005–1.01 g/mL while all of the protein was found at $d$ = 1.25 g/mL. Successful reconstitution was achieved (see Results) by using concentrations of detergent 5–10 times the cmc. We therefore used a detergent concentration of 100 mM for these studies. Once reconstituted, the vesicles were stored in buffer at 4 °C under argon, protected from light, and adjusted to pH 6.7. Successful reconstitution was obtained with octyl glucoside, but we were never able to obtain lipid to protein ratios of greater than about 100:1 with this detergent.

Recordings of light-induced pH changes were made with an Orion Model 601 digital pH meter equipped with an Orion Model 910300 pH probe. One-half milliliter samples were placed in a 12 × 35 mm plastic test tube that was clamped into a cylindrical 2-cm-bore jacketed glass vessel. A digital temperature probe (Bailey Instruments, Saddlebrooke, NJ) was kept in the sample to monitor temperature, which was held constant to ±0.2 °C by a circulating water bath. Output from the pH meter was stored in a Model 8000 Bascom Turner (Waltham, MA) microcomputer. Data were obtained at fixed intervals from 10 to 2500 ms. In the dark the pH recording apparatus was found to be stable to within 0.01 pH unit. To determine the response time of the system, we added an aliquot of 0.1 N NaOH or 0.1 N HCl to the vesicle solution with constant stirring to give a total pH change of 0.4 pH unit. The reading stabilized at the new value within 650 ms. All curves studied for analysis were recorded at sampling intervals of between 100 and 2500 ms. All data were stored on a floppy disk.

Illumination was accomplished with a 300-W bulb focused with a Kodak slide projector. Neutral density filters were used to control light intensity. Actual intensity was measured with a YSI-Kettering Model 65 radiometer calibrated with direct sunlight. No temperature or pH change was recorded when a vesicle preparation without BR was illuminated in identical buffer. Following each experiment, pH calibration curves were obtained by measuring the pH of the sample upon addition of known amounts of $10^{-3}$ M HCl and $10^{-3}$ M NaOH. Furthermore, knowing the size and concentration of the vesicles, we were able to calculate the percentage of the total volume contained within the vesicles. On the assumption that the intravesicular space displayed the same buffering as the external buffer, the amount of HCl or NaOH added in each calibration equaled the predicted accumulation of $H^+$ ions inside the vesicles during the greatest $H^+$ pumping observed. This allowed us to judge the approximate intravesicular pH change corresponding to the observed extravesicular change. At the largest pH change observed, the intravesicular pH was thus calculated to drop to between 5.1 and 5.7.

All data were transferred from the Bascom-Turner to a VAX 11/780 computer and analyzed with the CONSAM (conversational SAAM) program (Boston et al., 1981). Compartmental models were proposed to explain the observed kinetic patterns, and these were simulated on the computer by the appropriate differential equations contained within the program. The parameter values of the models were estimated by iteratively adjusting them until a least-squares fit of the data was obtained (Berman et al., 1962). Models were rejected when systematic deviations were still considerable after least-squares fitting. In addition to yielding least-squares estimates of parameter values, the CONSAM program also calculates estimates of variances and correlation coefficients for the parameters and for functions generated from the model solutions and the parameters. Details of the steps involved in deriving the proposed model for the observed kinetics are described later.

## Results

*Reconstitution.* Successful reconstitution resulted in a relatively uniform population of large unilamellar vesicles measuring approximately 1200 Å in diameter as shown by negative-stain electron microscopy. Vesicle size and uniformity were found to be independent of the protein to lipid ratio employed in reconstitution. The recovery of lipid after dialysis was variable and ranged from 40 to 80%. On the other hand 90–95% of the protein was consistently recovered. Isopycnic density centrifugation in KBr was used to determine the density and lipid to protein ratio of the recombinants (Figure 1). When lipid and protein were mixed at a molar ratio of 600:1, we recovered about 70% of the lipid. All of the lipid and protein cobanded at the top of the gradient (Figure 1B). The measured lipid to protein ratio in these pooled fractions was 450:1. When the original mixture was 100:1, the lipid and protein banded homogeneously toward the bottom of the gradient ($d$ = 1.2–1.25 g/mL), and the recovered lipid to protein ratio was 65:1 (Figure 1A).

In order to determine whether or not the above reconstitutions resulted in the incorporation of monomers, we examined the circular dichroism (CD) of the preparations in the visible range. Aggregation of BR monomers has been correlated with appearance of retinal exciton splitting (Heyn et al., 1975). Exciton splitting indicates pigment–pigment interaction but does not allow one to distinguish between dimer, trimers, or the presence or absence of a crystalline array. The visible CD spectrum of purified purple membrane sheets revealed the

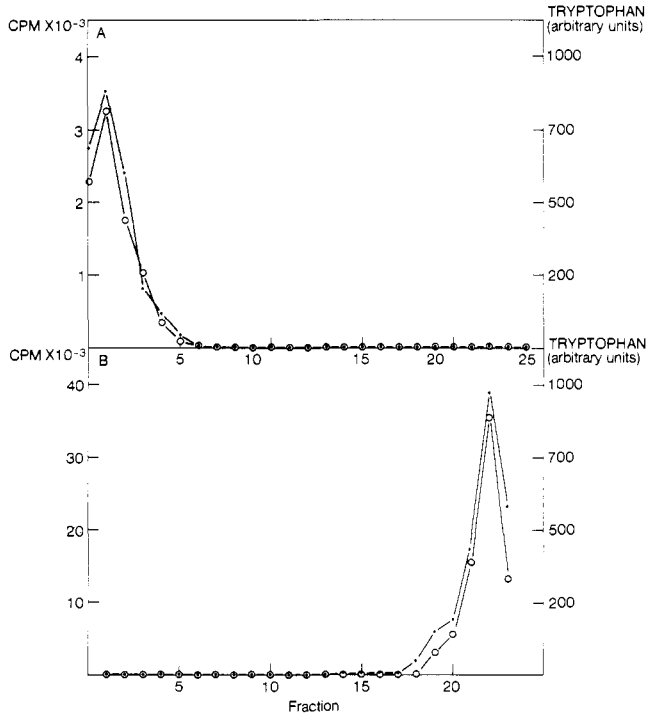


FIGURE 1: KBr density gradient from density 1.25 g/mL (at left) to 1.005 g/mL. The protein–lipid mixture was mixed with the heavy KBr solution, and the centrifugation was performed for 90 h at 4 °C in a Beckman SW50.1 rotor at 40 000 rpm. Four-drop fractions were collected by puncturing the bottom of the tubes and removing the gradient through a peristaltic pump. Open circles represent tryptophan fluorescence measured with a Perkin-Elmer Model 44B spectrofluorometer with $\lambda_{exc}$ 290 and $\lambda_{em}$ 340. [$^{14}$C]DPPC was measured by adding 2 mL of Hydrofluor (National Diagnostics) liquid scintillation fluid. In (A) is shown recombinants at a lipid to protein ratio of 65:1, and (B) shows the results at a ratio of 450:1.

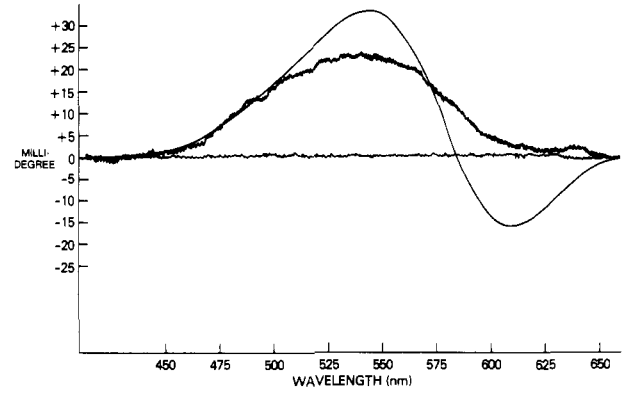


FIGURE 2: Visible circular dichroism of 450:1 (jagged line) and 65:1 (smooth line) BR–lipid recombinants, both at protein concentrations of 10 μg/mL. CD spectra were obtained with a Jasco (Japan Spectroscopy, Easton, MD) Model 500 spectropolarimeter. The purple membrane fragments used in this study showed an expected exciton splitting while the CHAPS-solubilized BR showed the single peak of positive ellipticity seen in the 450:1 lipid–protein recombinants.

characteristic exciton splitting. After solubilization with CHAPS, this is replaced by a single peak of positive ellipticity, consistent with the absorbance of the retinal. CHAPS itself has no optical activity in this region. This confirms that the solubilization procedure results in monomers of BR. In Figure 2 are shown the CD spectra of the high and low lipid to protein ratio recombinants, respectively. The vesicles with a lipid to protein ratio of 450:1 reveal a single, monomer peak while the exciton splitting is apparent in the 65:1 preparation. The CD spectra were corrected for scatter by subtracting contributions from the solvent and lipid-containing suspension and by varing the distance between the sample and the photomultiplier. The actual tracing revealing the flatness of the base line over the wavelength range and the extremely low noise is shown in Figure 2 for the monomer-containing vesicles. Although the detergent dialysis procedure, as outlined above, is straightforward and always resulted in the reconstitution of BR into vesicles, the exact results of each reconstitution were somewhat variable. We could select for monomer reconstitution by increasing the lipid to protein ratio, but this was not always successful and, in certain preparations, would result in exciton splitting. On two occasions, when high lipid to protein ratios were used, the result was two populations of vesicles, one with no detectable BR and exhibiting a density of 1.006 g/mL and one with a density of about 1.23 g/mL and containing BR that displayed exciton splitting. Thus it was very important to characterize each preparation according to density, lipid to protein ratio (determined from the gradient-purified recombinants), and CD.

*Pumping.* We examined the change in the pH of the medium by both the monomers and multimers in vesicles upon irradiation with light at 425 W/m$^2$. There was no qualitative difference between the two preparations in the extent of $H^+$ change. There was no change in pH in the dark. Upon illumination the pH in the extravesicular volume increased relatively rapidly over a period of about 50 s. When the light was turned off, there was a small rapid decrease in pH, followed by a slower return to the base line over 3–5 min. Although the figures do not show this, all curves did return to the initial preillumination pH. Once the pH returned to the initial value, repeated illuminations gave identical pH changes. Addition of the proton ionophore carbonyl cyanide *p*-(trifluoromethoxy)phenylhydrazone (FCCP) resulted in a loss of about 70% of the light-induced pH change. We were unable to abolish the entire pH change at any concentration of FCCP. Solubilization of the vesicles with Triton X-100, on the other hand, resulted in the total loss of light-induced pH change.

*Modeling.* We chose to model the kinetics of light-induced proton pumping using compartmental analysis. To illustrate the modeling process, we will use data obtained at 425 W/m$^2$ using multimeric recombinants. The pH as a function of time in the dark was monitored in all experiments so that any measured drift could be included in the modeling. The simplest model for removal of protons from the extracellular medium to the vesicles is given by

$$H_1 \underset{L(1,2)}{\overset{L(2,1)}{\rightleftharpoons}} H_2 \qquad (1)$$

where 1 and 2 represent the medium and vesicle, respectively, and $L(2,1)$ and $L(1,2)$ are rate constants for removal of protein from and back-flux into the intracellular medium. The single exponential derived from this exchange process could fit the initial rate of change of pH but not the obviously slower changes apparent at longer times of illumination nor the second, slower decay phase. This two-compartment model did not satisfactorily fit the data (Figure 3). We therefore introduced a second vesicle compartment 3, and in addition to the process described in eq 1, the process

$$H_1 \underset{L(1,3)}{\overset{L(3,1)}{\rightleftharpoons}} H_3 \qquad (2)$$

This model significantly improved the fit (Figure 4A). However, a small systematic error remained in all the fits. The initial parts of the "on" and "off" cycles fit the curves well, but the slopes of the latter portions of the calculated curves did not. In Figure 4A the systematic error is most obvious in the latter portion of the off curve. Any attempt to improve

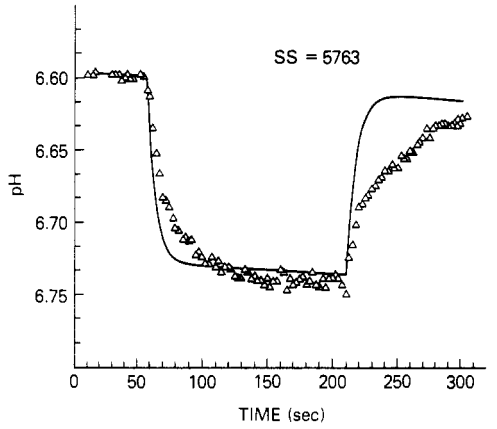


FIGURE 3: Two-compartment model in which initial rates of change of pH are fit for multimeric BR vesicles. Shown is the sum of the squares, which was calculated for nanomoles of $H^+$ ions rather than for pH.

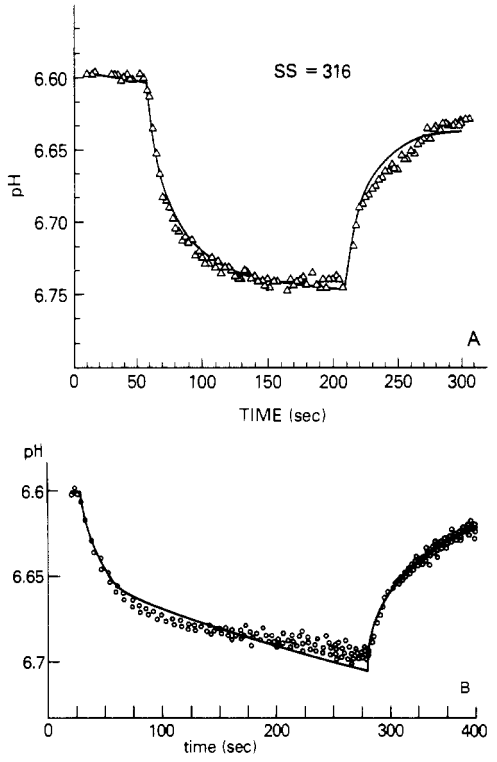


FIGURE 4: (A) Three-compartment model fit of data shown in Figure 3. (B) Fit of simple three-compartment model to a data set of multimeric BR vesicle pumping in which the fit to the off curve was manually maximized, showing the systematic error in the fit to the latter portion on the on curve.

the fit to the off curve resulted in a worsening fit to the latter portion of the on curve. Specifically when the decay curve is well fit by two exponential processes, the best fit of the initial rate of the slower on process overpredicts the actual pH change observed. An example of this is shown in Figure 4B. This systematic error was apparent in each of several dozen curves obtained with either monomeric or multimeric BR vesicles. This suggested that the two processes proposed to explain the pumping did not fully explain the data; in particular, it appeared that some additional factor was involved in limiting the rate of pumping of the second, slower process and that the extent of pumping was overpredicted by the initial rates. Not knowing what this was, we assumed that some phenomenon that occurred as a result of the pumping served to directly slow down or inhibit net pumping. A simple control function, $G(3)$,

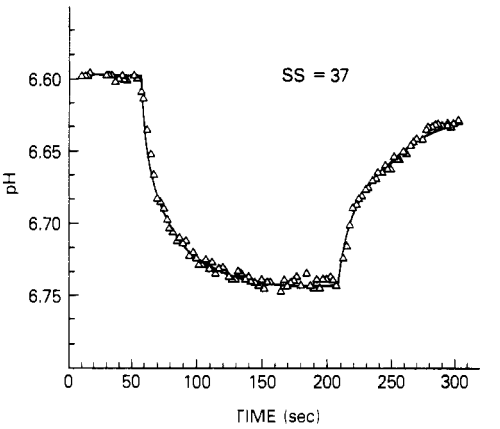


FIGURE 5: Fit of a three-compartment model with control function $G(3)$ to data shown in Figure 4.

was therefore introduced to limit the pumping rate. The function was made inversely dependent upon the amount of $H^+$ ions collected in compartment 3:

$$G(3) = 1/[1 + P(4)F(3)] \quad (3)$$

where $P(4)$ is a free variable and $F(3)$ is the amount of $H^+$ ions in compartment 3. The fit of the three-compartment model was greatly improved by this control function, and there were no remaining systematic errors observed for any set of experimental curves (Figure 5). The three-compartment model can be summarized by the rate of change of proton concentration in each compartment, $F(n)$:

$$dF(1)/dt = -L(2,1)F(1) - L(3,1)G(3)F(1) + L(1,2)F(2) + L(1,3)F(3) \quad (4)$$

$$dF(2)/dt = L(2,1)F(1) - L(1,2)F(2) \quad (5)$$

$$dF(3)/dt = L(3,1)G(3)F(1) - L(1,3)F(3) \quad (6)$$

Note that the control function, $G(3)$, is operating on the flow into compartment 3.

*Results of Three-Compartment Model.* We used the three-compartment model with the $G3$ control function to fit a series of experimental curves of light-induced pH changes as a function of irradiating intensity for both monomeric and multimeric bacteriorhodopsin vesicles (Figure 6). Excellent fits were obtained for all curves. Figure 7 shows the initial rate constants for the two on processes [$L(2,1)$ and $L(3,1)$] as a function of light intensity. Each process exhibits a linear dependency of rates on light intensity. Furthermore, as expected, the solutions of this model result in an intensity dependence that extrapolates to zero at zero light intensity. The rate constants for the processes are very similar for monomeric and multimeric vesicles although the data suggest that the rate constants are slightly greater for multimeric bacteriorhodpsin protein states. We tried numerous other models before accepting the one presented here. Clearly, a two-compartment exchange process did not fit the data (see Figure 3). Attempts to add a control function that would slow down the pumping of a single process also did not satisfactorily fit the data. We tried several variations on the three-compartment model either with or without the $G(3)$ control function. In one we attempted to yoke the fast and slow processes such that the former was required for the latter (a series model). With the $G(3)$ control function, this yielded reasonable fits to the experimental curves. However, the rate coefficients derived from such a series model varied randomly with light intensity and failed to suggest any extrapolation to zero proton movement at zero light intensity. Thus the combined criteria of good fits (with no systematic

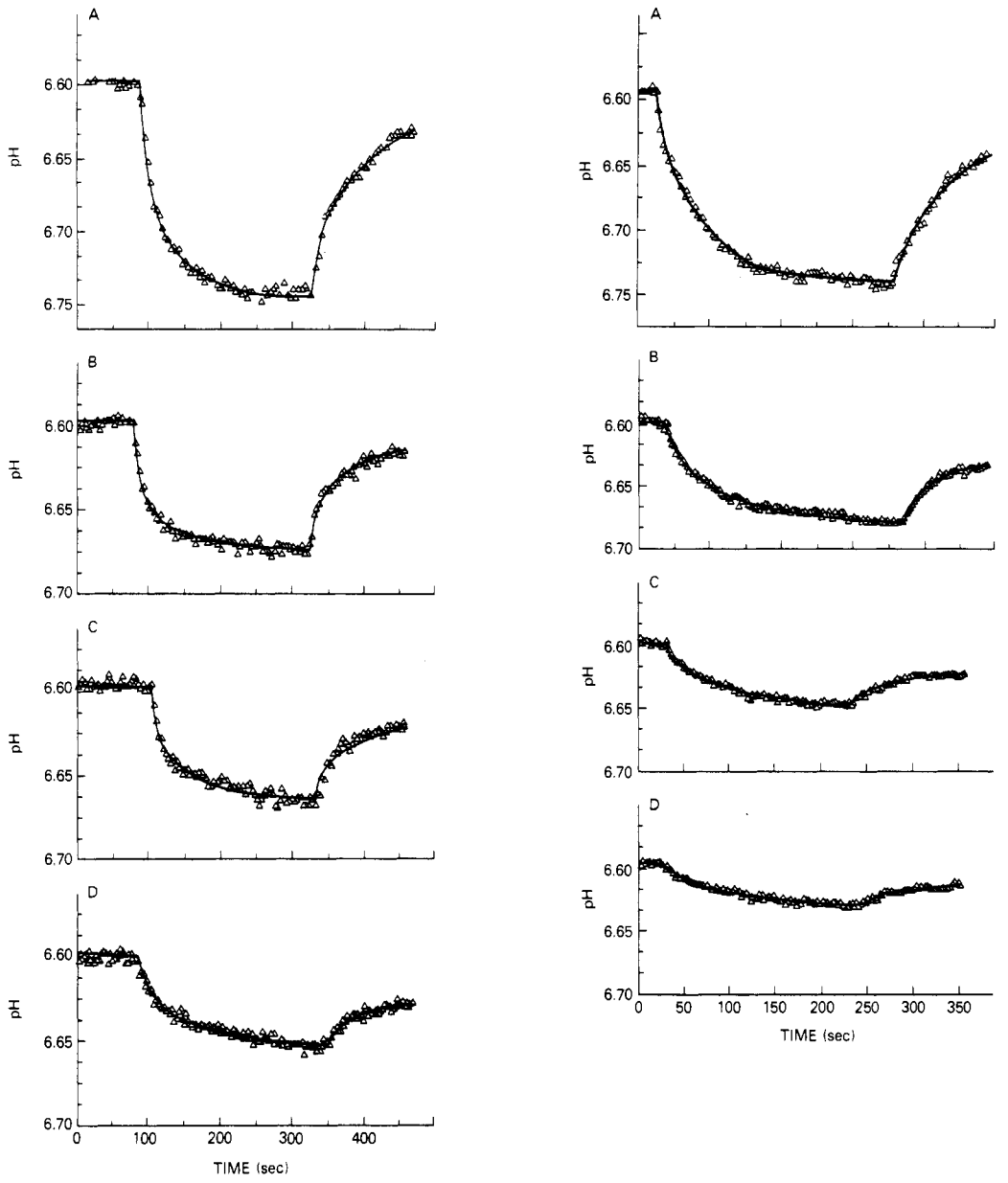


FIGURE 6: Observed data and theoretical curves according to model for multimeric (left panel) and monomeric (right panel) BR vesicles. Illumination at the following intensities is shown: (A) 425, (B) 325, (C) 175, and (D) 100 W/m$^2$.

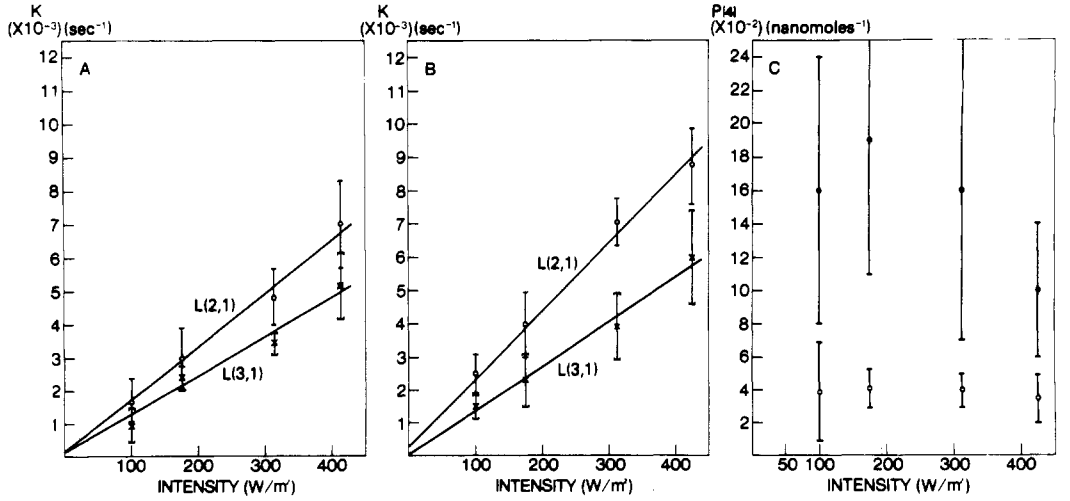


FIGURE 7: (A) $L(3,1)$ shown as (×) and $L(2,1)$ shown as (○) for monomeric BR vesicles as a function of light intensity. Error bars are estimated standard errors of the parameters derived from the least-squares fit of the model to the data. (B) As in (A) but for multimeric BR vesicles. (C) Values of $P(4)$ (see eq 3) for multimeric (●) and monomeric (○) BR vesicles.

errors) with meaningful relationships between light intensity and rate coefficients led us to accept the model presented here.

The values for $P(4)$ are shown in Figure 7C. This variable gives the proportionality factor of the influence of the amount of $H^+$ ions that have accumulated in compartment 3 upon the magnitude of the control function, $G(3)$. There is no apparent dependence of $P(4)$ on light intensity. Although poorly defined (i.e., note the standard deviations), it nevertheless is necessary to achieve a good fit of the data and serves as a crude indicator of some control or other, still unresolved processes. $P(4)$ for monomeric vesicles is significantly lower than for multimers. This would suggest that each pumped $H^+$ contributes less to the inhibition of pumping in monomers that in multimers. However, if we formulate $G(3)$ not in terms of the total amount of $H^+$ ions entering 3 [i.e., $=F(3)$] but rather in terms of the $H^+$ ions per vesicle, then the concentration in compartment 3 is increasing about 7-fold faster in the multimeric than the monomeric vesicles. This is so because there is a 7-fold higher vesicle concentration in the monomeric preparation. The corrected $P(4)$ of the monomers would be 7-fold higher than presently calculated. A 7-fold increase in the monomeric $P(4)$ would place the monomeric solutions within 1 standard deviation of the multimeric values for all intensities except the highest. This suggests that the inhibitory effect on pumping of the accumulation of $H^+$ ions per vesicle would be approximately of equal weight in both preparations. The decay or off reaction observed was excellently fitted to two single exponentials. Of note is the lack of dependence of these rate constants on light intensity. The finding that neither of the rate coefficients for the two off reactions varied with the amount of $H^+$ ions pumped is interesting in two respects. The lack of relationship between the rate coefficients and amount of ions pumped would be predicted for either a relaxation process or simple passive diffusion. Second, the model presented here assumes linear processes. The excellent fits suggest that the off reactions are consistent with such processes.

Steady-state values for the amount of $H^+$ ions pumped into each compartment were calculated from the model. This is accomplished by extrapolation of the curves to infinite time. For this calculation, as well as for all of the modeling, we are assuming that the protein is uniformly oriented. The reproducibility of the pumping between different preparations of either monomer or multimer is consistent with at least a highly reproducible orientation. Furthermore, we obtained identical results for the kinetics of proton movement using proteoliposomes from natural purple membrane sheets in which the orientation of the protein is likely to be homogeneous (Eisenbach et al., 1978). These values are shown in Figure 8. Not surprisingly the steady-state amount of $H^+$ ions in compartment 2 is linear with light intensity. However, the accumulation into compartment 3 shows a tendency to saturate at higher light intensities. This is a reflection of the control function that limits the amount pumped and is, itself, a function of the amount in compartment 3. The pumping is best expressed as $H^+$ ions pumped per protein monomer. It is clear that the capacities of compartments 2 and 3 are quite different and that the majority of $H^+$ transported is accounted for by compartment 3.

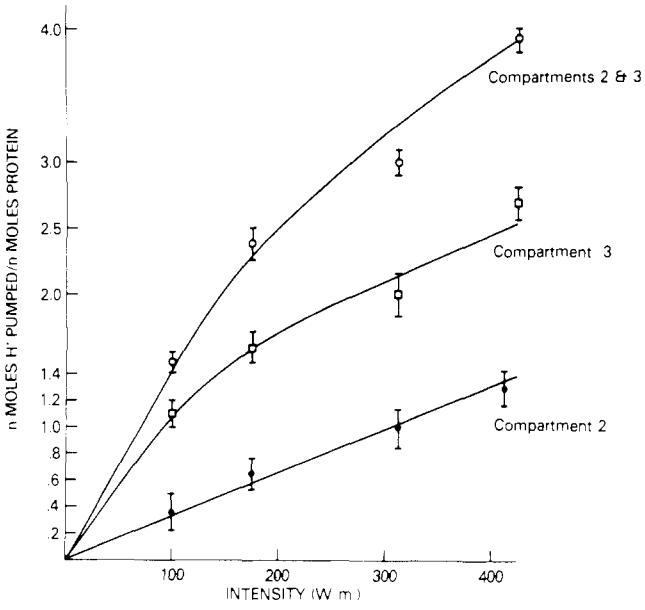


FIGURE 8: Steady-state accumulation of protons calculated as nanomoles of $H^+$ ions per nanomole of monomeric protein as a function of light intensity in multimeric BR vesicles. Shown are the accumulation into compartment 2 (●), compartment 3 (□) and the total (○).

## Discussion

Bacteriorhodopsin, both in multimeric and monomeric forms, can be reconstituted into phospholipid vesicles. These preparations exhibit light-induced proton pumping and can be used to study the detailed kinetics of the movement of protons. In order to use standard sums of exponentials to fit the pumping and decay curves simultaneously with common processes, one must impose initial conditions and constraints, and the choice of these constraints depends on the nature of the processes involved. It appears that there are only a few processes involved, and when these are directly modeled with compartmental analysis, there is a good chance, through various perturbation experiments, to deduce them. We were able to fit pumping and decay curves of both multimeric and monomeric bacteriorhodopsins at four different light intensities with a very simple three-compartment model. The failure to describe the data by a single process strongly suggests that at least two processes are involved in the light-induced movement of $H^+$ ions. Previously, Eisenbach et al. have described two processes in pumping of $H^+$ ions by subbacterial particles and proteoliposomes (Eisenbach et al., 1978, 1976). They proposed that the fast process did not actually represent "pumped" but "conformational" protons or Bohr protons. We have no direct experimental evidence concerning this point, but some aspects of the modeling results can be discussed in light of their proposal. The kinetics of the decay or off process in our study also reveal two exponential processes. The decay process most likely represents relaxation from the generated concentration gradient. Multiple leakage pathways from a single state, unless highly nonlinear, appear as a single process. We feel that the rapid off phase is therefore entirely consistent with a relaxation of the light-induced conformational change in BR proposed by Eisenbach to account for the rapid on phase. The magnitude of the proton shift due to such a mechanism would not be expected to surpass one or two protons per protein. The steady-state values for compartment 2 in our model are well within this range for all light intensities studied. If the rapid process indeed represents conformational protons, our compartment 2 is then most readily attributed to the protein itself. The rate constant associated with the uptake of protons into compartment 2 is relatively slow ($10^{-2}$ $s^{-1}$). It is clear that this process is much too slow to represent photocycle events, which take place at 100 Hz. If the "fast" process represents a slow light-induced conformational change of bacteriorhodopsin, it should be amenable to experimental confirmation.

It should be borne in mind that the rate-determining factor

in the steady-state translocation of protons is the permeability of the membrane to counterions and and co-ions, i.e., anions and cations coupled electrically to proton transport. It is readily shown that proton transport in our studies is essentially an electroneutral process, so that the development of the electrical potential difference across the membrane need not be explicitly considered in the kinetic calculations. The capacitance of a liposome is given by $C_{lip} = 4\pi K\epsilon_0 r_1 r_2/(r_2 - r_1)$, where we take the dielectric constant of the membrane, $K$, to have a value of 3, which is characteristic of lipid bilayers [see, for example, Hartmann et al. (1977)]. The permitivity of empty space, $\epsilon_0$, is $8.85 \times 10^{-12}$ F m$^{-1}$ (*Handbook of Chemistry and Physics*, 1981), the outer radius, $r_2$, is 60 nm in our liposomes, and the thickness of the bilayer, $r_2 - r_1$, is 4.57 nm (Cornell et al., 1980). Hence $C_{lip} = 2.43 \times 10^{-16}$ F. The number of protons pumped electrogenically is given by $N^e_{H^+} = C_{lip}\Delta\psi/e$, where the protonic charge $e$ is $1.59 \times 10^{-19}$ C and the membrane potential $\Delta\psi$ may be taken to be 75 mV in the multimeric liposomes (Kagawa et al., 1977). In the monomeric liposomes, where the lipid to protein ratio is much higher, $\Delta\psi$ is expected to be much lower. Hence, $N^e_{H^+} = 115$ for the multimeric liposomes, and this number may be considered an upper limit for the monomeric liposomes. To calculate the total number of protons pumped, $N^t_{H^+}$, we take the maximal proton accumulation at the highest light intensities used, $n_{H^+}$, to be 4 mol of $H^+$/mol of BR. The outer and inner surface areas per molecule of hydrated phosphatidyllecithin are 0.836 and 0.557 nm$^2$, respectively (Cornell et al., 1980). If the lipid to protein molar ratio is $\sigma$, then

$$N^t_{H^+} = 4\pi(r_1^2/0.557 + r_2^2/0.836)n_{H^+}/\sigma$$

Hence $N^t_{H^+} = 76\,000$ or 1100 for multimers or monomers, respectively. The fraction of pumped protons that are electrogenic is therefore 0.5% in the case of multimers and less than (probably considerably less than) 10% in the case of monomers.

Compartment 3, in our model, is most readily identified as the intravesicular space. The accumulation of $H^+$ ions into this compartment represents protons that have been pumped from compartment 1. The magnitude of accumulation in this compartment is greater than in compartment 2 (see Figure 8). The initial rate of entry of $H^+$ ions into this compartment is about half the initial rate into compartment 2. An additional feature of our model besides the clear demonstration of two processes is the control function, $G(3)$. We added this because of the finding of a systematic deviation in the data of the simple two-process model. The best fits of the initial rates resulted in a consistent overprediction of the amount of $H^+$ ions that entered compartment 3. The source of the inhibition may be the direct effect of the electrochemical potential upon the pump or of the intravesicle $H^+$ ion concentration itself. There is evidence that the pump is directly inhibited by the transmembrane electrochemical potential (Hellingwert et al., 1979). If the system were at equilibrium, microscopic reversibility would require that the control function, which limits the pumping rate, be compensated by an acceleration of $L(1,3)$. However, since $G(3)$ is modulating an active process, we need not expect the forward and reverse rate constants to be modulated proportionally. Although the indentification of our compartments with physical "compartments" is not straightforward in the absence of certain physical assumptions, the model we propose is beyond mere curve fitting. On the other hand, it does not yet provide a complete thermodynamic description of all the processes involved in light-induced proton movement.

Besides the extremely good fits of the model to all of the data sets, the results of the intensity dependence of the rate constants are worth noting. Light intensity was not included as a parameter in the model. However, the rate constants of both of the light-induced on processes showed a linear dependency upon light intensity. This is consistent with the analysis of Westerhoff et al. (1979). The extrapolation of both rate constants to zero at zero light intensity was a further encouraging result of the model. The results of the model show that only the two on rate constants are light-intensity dependent. This study supports the findings of Eisenbach et al. (1978) in that the light-induced movement of $H^+$ ions appears to involve two first-order processes. Our model portrays these two processes as parallel and independent. Although this model fits the numerical data, we cannot rule out the possibility that these two processes are interdependent.

There is no major difference between the pumping kinetics of multimeric and monomeric bacteriorhodopsin. This finding is consistent with the report by Dencher & Heyn (1979) that both form the protein pump. Our results leave unanswered the teleological question of why the protein assumes the crystalline array in which it is found in nature (Henderson & Unwin, 1975). It is, however, conceivable that the multimeric form is more efficient at establishing and maintaining a transmembrane $H^+$ ion gradient. Our preparations of multimeric protein had about 7-fold fewer vesicles than the monomeric preparations. Despite this, the number of $H^+$ ions removed from the medium was comparable for each preparation, and thus the transmembrane $H^+$ ion gradient was about 7 times greater in the multimeric peparation. More direct demonstration of altered pumping efficiency is required before any difference between monomeric and multimeric bacteriorhodopsins will be established.

## References


Berman, M., Shahn, E., & Weiss, M. F. (1962) *Biophys. J. 2*, 275.

Bogomolni, R. A., & Stoeckenius, W. (1974) *J. Supramol. Struct. 2, 775.*

Boston, R., Greif, P., & Berman, M. (1981) *Comput. Programs Biomed. 13*, 111.

Cornell, B. A., Middlehurst, J., & Separovic, F. (1980) *Biochim. Biophys. Acta 598*, 405.

Dencher, N. A., & Heyn, M. P. (1979) *FEBS Lett. 108*, 307.

Eisenbach, M., Bakker, E. P., Korenstein, R., & Caplan, S. R. (1976) *FEBS Lett. 71*, 228.

Eisenbach, M., Garty, H., Bakker, E. P., Klemperer, G., Rottenberg, H., & Caplan, S. R. (1978) *Biochemistry 17*, 4691.

*Handbook of Chemistry and Physics* (1981) 62nd ed., p F203, CRC Press, Boca Raton, FL.

Hartmann, R., Sickinger, H.-D., & Oesterhelt, D. (1977) *FEBS Lett. 82*, 1.

Hellingwert, K. J., Scholte, B. J., & Van Dam, K. (1978) *Biochim. Biophys. Acta 513*, 66.

Hellingwert, K. J., Arents, J. C., Scholte, B. J., & Westenhoff, A. V. (1979) *Biochim. Biophys. Acta 547*, 561.

Henderson, R. (1977) *Annu. Rev. Biophys. Bioeng. 6*, 87.

Henderson, R., & Unwin, P. N. T. (1975) *Nature (London) 257*, 28.

Heyn, M. P., Bauer, P.-J., & Dencher, N. A. (1975) *Biochem. Biophys. Res. Commun. 67*, 897.

Kagawa, Y., Ohno, K., Yoshida, M., Takeuchi, Y., & Sone, N. (1977) *Fed. Proc., Fed. Am. Soc. Exp. Biol. 36*, 1815.

Marcus, M. A., & Lewis, A. (1977) *Science (Washington, D.C.) 195*, 1328.

Oesterhelt, D., & Hess, B. (1971) *Eur. J. Biochem. 37*, 316.

Oesterhelt, D., & Stoeckenius, W. (1971) *Nature (London), New Biol. 233*, 149.
Oesterhelt, D., & Stoeckenius, W. (1973) *Proc. Natl. Acad. Sci. U.S.A. 70*, 2853.
Oesterhelt, D., & Stoeckenius, W. (1974) *Methods Enzymol. 31*, 667.
Racker, E. (1973) *Biochem. Biophys. Res. Commun. 55*, 224.
Racker, E., & Stoeckenius, W. (1974) *J. Biol. Chem. 249*, 662.
Slifkin, M. A., & Caplan, S. R. (1975) *Nature (London) 253*, 56.
Westerhoff, H. V., Scholte, B. J., & Hellingwert, K. J. (1979) *Biochim. Biophys. Acta 547*, 544.

# Resolution and Activity of Adenylate Cyclase Components in a Zwitterionic Cholate Derivative [3-[(3-Cholamidopropyl)dimethylammonio]-1-propanesulfonate]†

Alan J. Bitonti,‡ Joel Moss,* Leonard Hjelmeland, and Martha Vaughan

ABSTRACT: Bovine brain adenylate cyclase was solubilized with 3-[(3-cholamidopropyl)dimethylammonio]-1-propanesulfonate (CHAPS), sodium cholate, sodium deoxycholate, or these detergents plus $(NH_4)_2SO_4$. The specific activity of the extract obtained with 13 mM CHAPS alone was several times those of the other detergent extracts with or without $(NH_4)_2SO_4$. After solubilization with 13 mM CHAPS, gel filtration completely separated the catalytic unit (C) from the guanine nucleotide binding protein (G/F). C activity when assayed with 5 mM $Mn^{2+}$ was 5 times that assayed with 10 mM $Mg^{2+}$ and was unresponsive to GPP(NH)P. C activity was increased ~150% by GPP(NH)P in the presence of G/F extracted from human erythrocyte ghosts and ~100% by $Ca^{2+}$ plus calmodulin in assays with $Mg^{2+}$. On gel filtration and/or density gradient centrifugation, the physical properties of C from brain or $AC^-$ cells and G/F from bovine or pig erythrocytes in CHAPs were similar to those observed in other detergents. It appears that the use of CHAPS for solubilization of adenylate cyclase and separation of C and G/F may well prove advantageous in studies of the molecular interactions between the protein subunits and activators of the enzyme as well as for the initial purification of C.

Hormone-sensitive adenylate cyclase is believed to consist of at least three protein components: a hormone receptor, the catalytic unit (C),[1] and a guanyl nucleotide binding protein (G/F). To study the regulatory interactions of the proteins, it is desirable to be able to separate each component from the others and subsequently reassemble them in artificial membranes. Other workers have separated C and G/F by extraction of plasma membranes with sodium cholate and high concentrations of $(NH_4)_2SO_4$, followed by gel filtration of the extracts (Strittmatter & Neer, 1980; Ross, 1981). High concentrations of $(NH_4)_2SO_4$, however, change the properties of cholate and are also severely inhibitory to adenylate cyclase. It would be advantageous to separate C and G/F in the absence of the salt.

The zwitterionic detergent CHAPS (Hjelmeland, 1980) was recently introduced as an alternative to both ionic detergents, such as cholate (Hoffman, 1979; Strittmatter & Neer, 1980; Ross, 1981) and deoxycholate (Londos et al., 1979; Hebdon et al., 1981), and nonionic detergents, such as Lubrol (Haga et al., 1977; Neer et al., 1980) and Triton (Neer et al., 1980), all of which have been used for solubilization of adenylate cyclase. We compared the effectiveness of CHAPS, sodium cholate, and sodium deoxycholate or these detergents plus $(NH_4)_2SO_4$ for solubilization of bovine brain adenylate cyclase and found that CHAPS was significantly better than either of the bile salts for dispersing adenylate cyclase from brain particulate fractions. As reported here, the use of CHAPS for solubilization of adenylate cyclase from bovine brain allows the separation of C from G/F by gel filtration, and in CHAPS the hydrodynamic properties of both C and G/F correspond quite closely to values obtained with other detergents.

## Experimental Procedures

*Solubilization of Brain Adenylate Cyclase.* Fresh bovine brain was stored at −70 °C. For each experiment, a small piece of cortex was removed, thawed in cold 50 mM glycine buffer, pH 8.0, and homogenized by hand in 5 volumes of the same buffer. The homogenate was centrifuged for 10 min at 15000*g*. The pellet was washed twice with 20 volumes of 50 mM glycine (pH 8.0) containing 0.5 mM EGTA and once with 10 volumes of 50 mM glycine, pH 8.0 (with centrifugation at 30000*g* after each wash), and dispersed in the same buffer (final protein concentration 2 mg/mL). Detergent was added as indicated, and after 30 min on ice the mixture was centrifuged at 100000*g* for 60 min; the supernatant contained the solubilized adenylate cyclase.

*Preparation of $AC^-$ Membranes and Solubilization of C.* $AC^-$ cells, kindly provided by Dr. Alfred G. Gilman, were grown at 37 °C in Dulbecco's modified Eagle's medium

† From the Laboratory of Cellular Metabolism, National Heart, Lung, and Blood Institute (A.J.B., J.M., and M.V.), and the Developmental Pharmacology Branch, National Institute of Child Health and Human Development (L.H.), National Institutes of Health, Bethesda, Maryland 20205. *Received October 20, 1981.*
‡ Present address: Merrell-Dow Pharmaceuticals, Cincinnati, OH 45215.

[1] Abbreviations: C, catalytic unit; G/F, guanyl nucleotide binding protein; CHAPS, 3-[(3-cholamidopropyl)dimethylammonio]-1-propanesulfonate; EGTA, ethylene glycol bis(β-aminoethyl ether)-*N,N,N′,N′*-tetraacetic acid; Hepes, 4-(2-hydroxyethyl)-1-piperazineethanesulfonic acid; APP(NH)P, 5′-adenylyl imidodiphosphate; GPP(NH)P, guanylyl imidodiphosphate; EDTA, ethylenediaminetetraacetic acid; Tris, tris(hydroxymethyl)aminomethane.